

PACS numbers: 52.57.Bc; 52.38.Dx; 52.50.Nr
DOI: 10.1070/QE2003v033n11ABEH002531

On the possibility of high-temperature plasma production by laser pulses irradiating a volume-structured medium formed upon the explosion of a thin conductor

S.Yu. Gus'kov, G.V. Ivanenkov, S.A. Pikuz, T.A. Shelkovenko

***Abstract*. The properties and parameters of volume-structured metal media produced by exploding thin conductors in a high-power electric discharge are analysed. Such media are proposed for the production of nonequilibrium high-temperature laser plasma as a high-power X-ray and neutron radiation source. The physics of the interaction of a high-power laser pulse with a volume-structured metal medium and the properties of produced nonequilibrium plasma are considered.**

Keywords: *laser plasma, porous media, electric discharge.*

1. Introduction

In recent years, the emphasis in high-power laser radiation–matter interaction studies is placed on new types of targets containing low-density volume-structured media. The internal structure of these media may be either regular or random. A typical example of a regular structure is a system of thin layers of a solid with vacuum spaces between them. Stochastic porous structures may be structurally fibrous, foamy, or finely dispersed. The structures of primary interest are those whose average density is close to or exceeds the critical density of laser plasma*. The interest in studies of the interaction of laser radiation with volume-structured media arises from the possibility of employing them as an efficient absorber of laser radiation in laser fusion targets [1]. Such an absorber is capable of smoothing out the nonuniformities of target heating driven by the laser beams. In the near future, the development of new types of pulsed neutron [2] and X-ray [3, 4] radiation sources based on such media can be expected.

The most important processes of the interaction of laser radiation with a porous medium, which define the features of laser radiation absorption and plasma production, are as follows [3]. The light penetrates into the target by a distance equal to the geometric transparency depth to give rise to volume radiation absorption. The heating and evaporation of the solid elements of the target structure in the absorption region results in the collision of plasma streams and the generation of shock waves. The interaction of these streams and shock waves leads to the homogenisation of the medium, which proceeds in two stages. The first stage involves the initial filling of the medium cells with the vaporised material of the solid elements. For a laser radiation intensity of $10^{13} - 10^{15}$ W cm^{-2}, the duration of this homogenisation stage for porous media with pore dimensions of 30 – 100 μm is equal to several hundreds of picoseconds. The second homogenisation stage involves viscous dissipation in the collision of plasma streams and shock waves. Its duration is quite long and may range, under the above conditions, from several nanoseconds to several tens of nanoseconds.

During the homogenisation, the state of the laser plasma of porous media is nonequilibrium, with temporal and spatial oscillations of the plasma ion temperature and density occurring in it. The long duration of this process for a porous material with a near-critical average density gives rise to several very important properties of the laser plasma. For the porous media of light elements, the majority of these properties have been experimentally confirmed at laser radiation intensities $10^{13} - 10^{15}$ W cm^{-2}. The most important of these properties are as follows.

(i) The absorption coefficient for laser radiation amounts to 80 % – 100 %, including porous materials with an average density exceeding the critical one by an order of magnitude, and depends only slightly on the angle of laser radiation incidence [5 – 8].

(ii) Regular reflections and refractions of light are absent [5, 6].

(iii) The radiation is absorbed at the geometric transparency depth

$$L_{ab} \approx C\left(\frac{\rho_s}{\rho_a}\right)^{1/2} b_0, \qquad (1)$$

which corresponds to the dimension of the partially homogenised region of the porous material [6]. Here, ρ_s and ρ_a are the characteristic densities of the porous material in the normal state, ρ_s is the density of an individual solid element, and ρ_a is the average density of the target material; C is a constant equal to 14.8 for a material with a fibrous structure (agar – agar, etc.) and to 12.1 for a material with a honeycomb structure (porous polystyrene and polypropy-

*In units of g cm^{-3}, the critical plasma density is defined by the formula $1.83 \times 10^{-3}(A/Z)\lambda^{-2}$, where A and Z are the atomic weight and the average ion charge, and the wavelength λ is measured in μm. For the $\lambda = 1.06$ μm radiation, the critical density for plasmas with multiply charged ions ranges from 3.6×10^{-3} g cm^{-3} for the ratio $A/Z \approx 2$ (full ionisation) to 1.8×10^{-2} g cm^{-3} for $A/Z \approx 10$ (typical heavy metal plasmas).

S.Yu. Gus'kov, G.V. Ivanenkov, S.A. Pikuz, T.A. Shelkovenko
P.N. Lebedev Physics Institute, Russian Academy of Sciences, Leninskii prosp. 53, 119991 Moscow, Russia

Received 20 February 2003
Kvantovaya Elektronika **33** (11) 958 – 966 (2003)
Translated by E.N. Ragozin

lene); and b_0 is the least characteristic dimension of the structure elements.

(iv) The transfer of absorbed laser radiation energy occurs due to the propagation of the so-called hydrothermal wave. Its velocity is close to the shock wave velocity in a homogeneous material with a density equal to the average density of the porous medium, and the temperature distribution behind the shock front is nearly uniform due to its rapid equilisation by electron thermal conduction. In the laser plasma of porous media with a near-critical density, the velocity of energy transfer is equal to $(1-2)\times 10^7$ cm s^{-1} [5–8].

(v) In the course of homogenisation, the plasma proves to be in a nonequilibrium state with strongly different ion (1.5–2 keV) and electron (0.5–0.7 keV) temperatures [6]. In this case, inside the cells there occurs multiple conversion of the thermal energy of plasma streams to kinetic energy, and the porous material accumulates internal energy almost without any expansion. Intense expansion begins after the completion of homogenisation, and it is close to a thermal explosion in character [5–8].

The formation and prolonged existence of a nonequilibrium high-temperature plasma offers strong possibilities of investigating basic plasma processes, including the relaxation, ionisation, and radiative ones. Introducing deuterium and (or) tritium into such media makes it possible to produce nonequilibrium laser plasma with a nearly fusion ion temperature and generate in it high-power neutron pulses [2]. Finally, the laser plasma of volume-structured media containing heavy elements serves as a source of soft X-rays, providing under certain conditions a high conversion efficiency of laser radiation to X-rays (close to 70 %–80 %) [4].

The application of picosecond and femtosecond ultrahigh-intensity ($I > 10^{16} - 10^{17}$ W cm^{-2}) laser pulses opens up interesting possibilities for investigations in this direction. One of the examples is experiments with finely dispersed media produced when the vapour of some material expands through a nozzle and cools down. In these experiments, megaelectron-volt electrons and ions were detected, whose energies correspond to the Coulomb explosion of the clusters of the medium heated by the laser pulse, and also high-power neutron pulses and other effects described in Ref. [9].

In this paper, we propose to use metals in a foamy or droplet state produced by a high-power vacuum electric discharge through thin conductors as a volume-structured medium for laser-plasma production.

2. Properties of a metal volume-structured medium produced by an electric discharge through a thin conductor

Recent experiments carried out at Cornell University [10, 11] (in what follows these data are refined below based on the latest results) with the participation of two authors of our work, S.A. Pikuz and T.A. Shelkovenko, have revealed the following. At the initial stage of a nanosecond explosion of conductors during resistive heating there occurs a rapid energy input, which is determined by the physical properties of the metal, the parameters of the current circuit, and experimental conditions. At the next stage there occurs the explosion itself and the material transforms to a two-phase liquid-vaporous state: a greater part of the material forms a dense core, which typically has the structure of a foam with a sharp external boundary [12, 13], with a corona emerging outside of the foam. A sharp rise of the load impedance is observed during the explosion, and the corona, which is formed form the material vaporised from the surface prior to the explosion, rapidly transforms to a plasma and then shunts the current flowing through the core. This abruptly interrupts the energy input into the core, and subsequently the current flows almost entirely through the corona.

The subsequent behaviour of the core essentially depends on the ratio between the energy deposited into the material and the expenditure of heat for melting and evaporation. Experiments for a current build-up rate of $(1-2)\times 10^{10}$ A s^{-1} showed [10] that the melting energy is easy to exceed for all metals, while the evaporation energy can be achieved only for low-melting well-conducting metals (Al, Cu, Ag, Au) under special conditions. The core has usually a heterogeneous structure, which is determined by the thermal and electrical properties of the metal and the time elapsed from the onset of discharge up to the current shunting.

The core structure was investigated by laser probing and X-ray radiography techniques (in the latter case, an *X*-pinch was employed as the radiation source [14]). A simplified layout of the experiment is shown in Fig. 1. The wires exploded in a vacuum diode (*1*) with a gap of 10–15 mm, its electrodes were connected to a low-inductance capacitor-based current generator via a short coaxial cable [10]. The current had the form of a decaying sine curve with the amplitude up to 4.5 kA and the first peak at 350 ns. During the first 100 ns of the discharge, the current showed special features related to the phase of ohmic wire heating (see Ref. [10]).

Optical schlieren photographs and interference patterns of the wires were recorded using the second harmonic radiation of a Nd:YAG laser with a pulse duration of 4 ns (Fig. 1). We used an interferometer with an air wedge based on a two-prism beamsplitter [15]. The spatial resolution was 50–100 μm, which was considerably inferior to

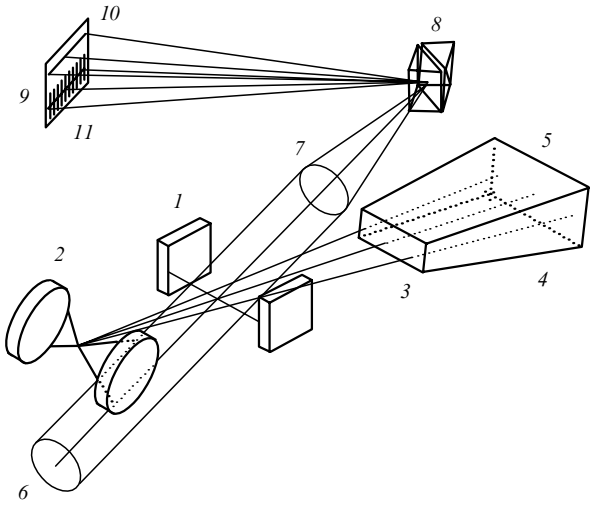

Figure 1. Scheme of the exploding-wire experiment: (*1*) diode gap with a wire under study; (*2*) diode gap with an *X*-pinch; (*3*) titanium filter; (*4*) screened camera; (*5*) X-ray photographic film; (*6*) laser beam; (*7*) lenses; (*8*) beamsplitter wedges; (*9*) photographic film; (*10*) shadowgraph; (*11*) interference pattern.

resolution of the X-ray technique. X-ray images of the wire were obtained by illuminating it with the radiation of the *X*-pinch, a 12.5-μm thick titanium filter blocking the photographic film from visible and ultraviolet radiation. To broaden the sensitivity range, the screened camera was loaded with a batch of three films, each preceding film serving as an additional filter for the next ones. The films were arranged according to their sensitivities: Mikrat VE was the first, Kodak DR was the second, and Kodak DEF – the third. Considering the spectral sensitivities of the photographic films and the transmittance of the filter, the film substrate, and the photographic emulsions, the wavelength range being recorded was 2.5 – 5 Å for the first photographic film, 2.5 – 3.5 Å for the second, and 1 – 2 Å for the third. We used the dot projection technique, whose spatial resolution is determined by the dimension of the emission region and X-ray diffraction. The size of an individual radiating hot dot did not exceed 1 – 2 μm, the diffraction limit was 2.5 – 5 μm, depending on the wavelength. The images were digitised with the help of a Nikon LS-2000 slide scanner with a resolution of 2700 dots per inch (dot size was 9.4 μm). Taking the geometrical magnification into account, this corresponded to a resolution of 2.1 μm. Thus, the overall spatial resolution, for example, for the second photographic film was no worse than 5 μm. The time resolution was determined by the exposure time – the X-ray burst duration, which did not exceed 50–100 ps. The energy deposited into the wire was determined by integrating the power of current flowed through the wire up to the instant of shunting [10].

The optical and X-ray discharge photographs for copper, silver, and gold are shown in Fig. 2 and for tungsten in Fig. 3. Three regions are well distinguished in the optical range: a dense core opaque for the laser radiation (in the figures, its diameter is 10 – 30 times larger than the initial wire diameter, depending on the material, the expansion velocity is 0.1 – 0.5 μm ns^{-1} [10]) and a 0.1 – 0.5 mm thick vapour layer around the core, which grades into the plasma (the change of fringe shift direction in the interference patterns).

The core opacity cannot be attributed simply to the refraction of the laser beam caused by a strong gradient of the refractive index and the beam escape from the aperture of the optical system. The interference fringes at the core boundary vanish in a jump-like manner without being condensed, as would normally be the case if the medium were transparent. The aperture of the optical system allowed us to observe shifts by 5 – 7 fringes. Note that the fringes were sometimes observable against the background of the core as well, but this took place only when it was possible to deposit into the wire an energy sufficient for its complete evaporation. In our case, the core opacity therefore corresponds to the absorption or scattering of laser radiation in the heterogeneous core.

The core structure and the character of its inhomogeneities are revealed with the help of X-ray radiography. The penetration depth of X-rays is determined by its hardness and the object material, while the attenuation of incident radiation is proportional to the mass of material along the beam path and is independent of its aggregate state, whether it be solid, liquid, gas, or not-too-strongly ionised plasma. This permits obtaining the values of column density along the rays by comparing X-ray absorption in the discharge material with the absorption of a layer of the same metal of a given thickness [16]. Step attenuators were evaporated directly on the titanium filter, which protected the photographic film. The sensitivity range of this technique exceeds two orders of magnitude, which corresponds to a metal thickness under normal conditions from 0.01 – 0.05 to 2 – 10 μm, depending on the chemical composition. The intersection of the sensitivity ranges of the optical and X-ray techniques allows one to measure also the vapour polarisability and the ionisation state of a plasma.

In X-ray images (Figs 2 and 3), the dense core in place of the optically opaque region is embedded in a medium whose density gradually decreases towards the periphery transparent in the visible light. The optically opaque core carries the bulk of exploded wire mass. The values of energy deposited into the wires, the heat of melting and evapo-

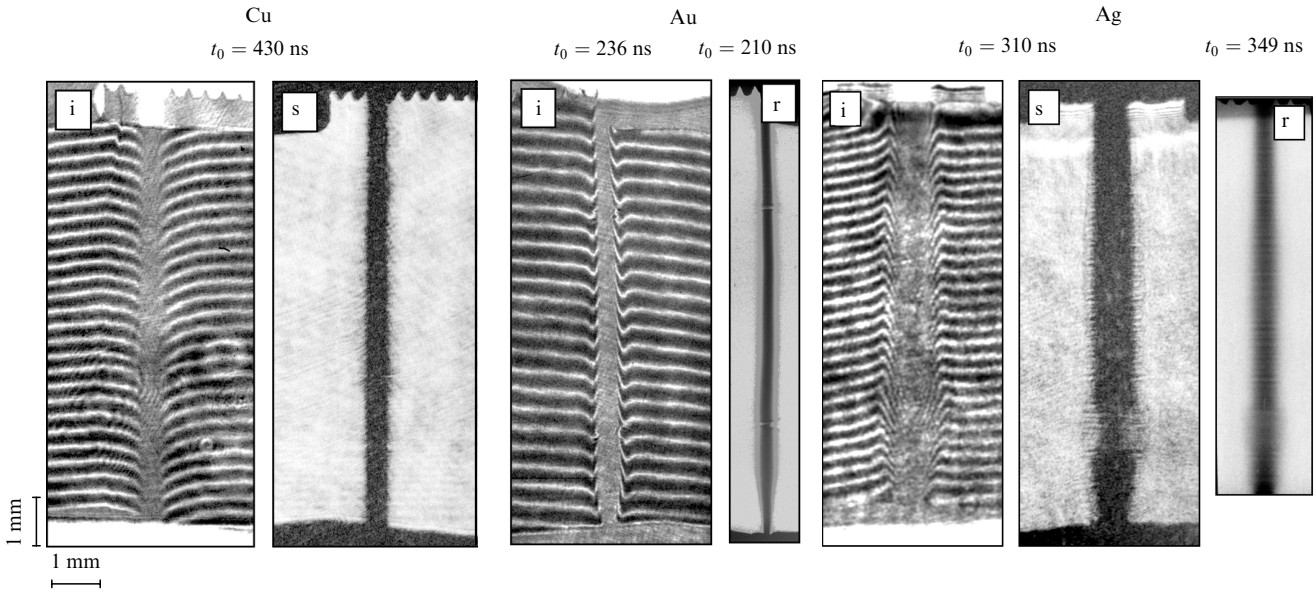

Figure 2. Optical interference patterns (i) and shadowgraphs (s) as well as X-ray photographs (r) of discharges through the wires of Cu (∅25 μm), Au (∅20 μm), and Ag (∅25 μm). The instants of exposure t_0 measured from the onset of current are indicated by the photographs. The interference patters show positive (downward) and negative (upward) fringe shifts caused respectively by the vapour and the plasma.

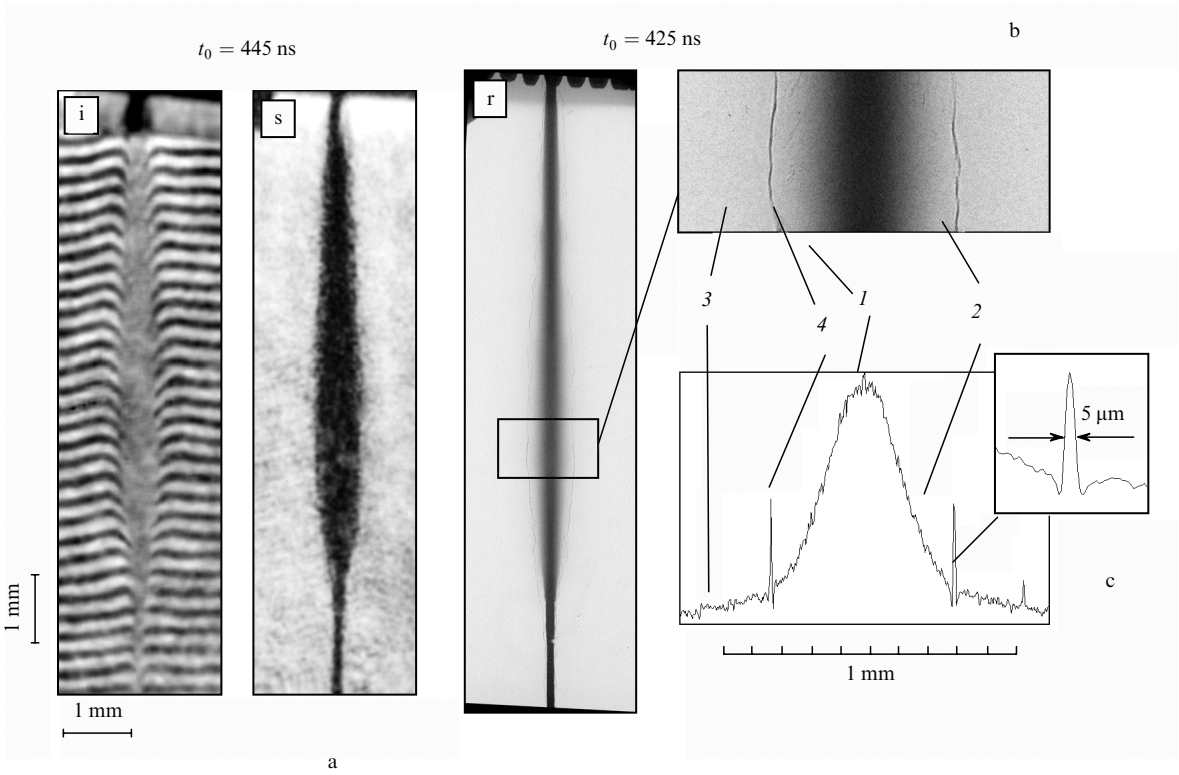

Figure 3. Optical (t_0 = 445 ns) and X-ray (t_0 = 425 ns) photographs of discharge through tungsten wires (∅25 μm) in an insulating shell (polyimide) (a). The magnified fragment (b) of the last photograph and densitogram given below (c) show the region of core (*1*), vapour, and droplets (*2*), of plasma (*3*), as well as the polyimide film (*4*). The notation is the same as in Fig. 2.

Table 1.

Material	Diameter/μm	Energy deposition/mJ	Melting energy/mJ	Evaporation energy/mJ	Energy deposition/ evaporation energy
Cu	25	88 – 112	28	251	0.37 – 0.47
Ag	25	76 – 112	20	138	0.55 – 0.61
Au	20	55 – 60	14	113	0.49 – 0.71
W	25 (+ 5 μm insul.)	120 – 210	42	432	0.28 – 0.49

ration for the materials under discussion (for more details, see Ref. [10]) are collected in Table 1. A circumstance significant for the further discussion follows from Table 1: the energy deposition is significantly greater than the melting heat but is nevertheless sufficient for the evaporation of only a part of the wire mass. The remaining part of the material should be liquid. In the limit, the 'exploded' metal can form a foam with an average density of 1 % – 10 % of the solid density (this supposedly take place in the dense core, where the characteristic size of the foam cells does not exceed 20 – 30 μm; the size of the boundary films turns out to be at the limit of or smaller than the spatial resolution) or a cloud of droplets with an average density of 0.1 % – 1 % of the same quantity.

Of special interest are metal droplets formed in the process. Early in the process (for $t < 1$ μs), their dimension is below the spatial resolution limit and they do not show on Figs 2 and 3, but a rather sharp boundary of the opacity region is indication that their fraction is not small. At later discharge stages ($t > 1$ μs), when there is scarcely any current through the gradually expanding core, inside the core there occurs transformation of liquid films to droplets. At a later stage, the vapour, which cools down due to expansion, also condenses to droplets. As to the interaction of the liquid core component with the surrounding vapour, which has a low heat conductivity, and the radiation arriving from the plasma corona, they cannot have a significant effect on the fate of the droplets. It is well known [12] that even a high-current discharge*, which heats the corona up to temperatures of the order of 100 eV, retains a cool and dense core inside. Under our experimental conditions, in view of the data of Ref. [16] that only ~ 10 % of the material passes into the corona, the Bennett estimate yields a coronal temperature of only about 1 eV. The core heating by the corona is therefore extremely weak, and after a sufficiently long period of time all the material should find itself in a droplet-vaporous state. Finally, the evaporation of droplets, even in circumstances where the liquid – vapour

*The discharge was simulated in papers [10, 11]. In all the cases under consideration, there occurs one and the same type of electric conductor explosion – the so-called rapid explosion, when the Joule heat proceeds faster not only than the development of magnetohydrodynamic instability of a melted wire, but also than the shorter process of rarefaction penetration to the wire axis.

equilibrium is absent, does not lead to a significant reduction of their size, unless the temperature attains a value close to the critical one. Furthermore, lots of fine particles of the 'exploded' metal were repeatedly found after a 'shot'. All this testifies to the persistence of condensed phase up to the termination of discharge.

The resultant droplets are clearly seen near the electrodes (Fig. 4). The Fourier analysis of the images shows that their average size ranges between 6 and 10 μm, while at the diode centre it is only slightly greater than the 3–5 μm characteristic resolution limit. The presence of droplets is clearly demonstrated in the explosion of two parallel golden wires: it is evident from the X-ray images (Fig. 4) that the wire core remnants expand independently to interpenetrate showing no signs of interaction. This testifies to the ballistic nature of the motion of droplets and to their large fraction in the mixture. Otherwise the X-ray images and the interference patterns would have shown a compression generated by the collision of two counter-expanding masses like, for instance, in the explosion of a pair of silver wires (Fig. 5). Note that silver was always found to be close to complete vaporisation.

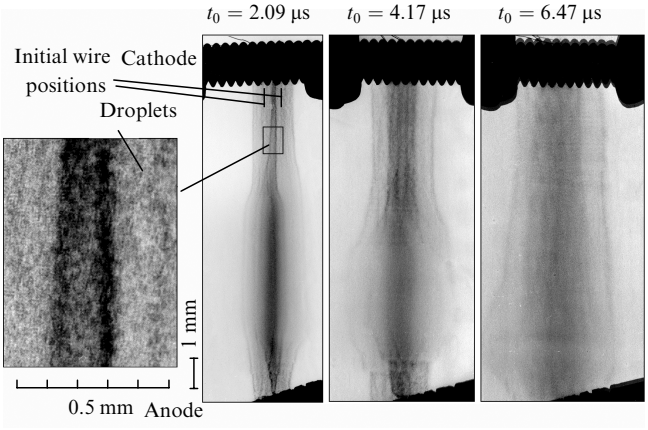

Figure 4. X-ray photographs of exploded gold wires (∅20 μm) in three 'shots' at different points in time.

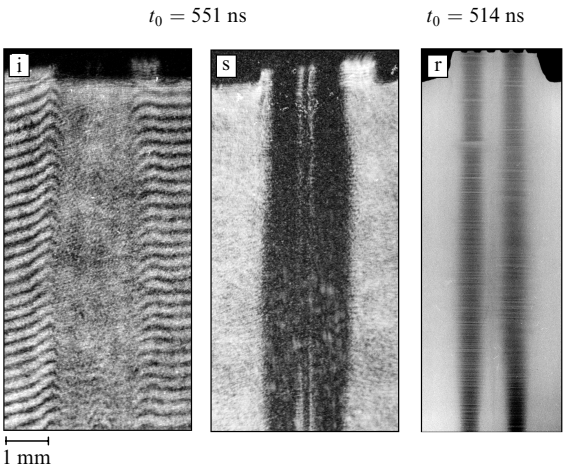

Figure 5. Photographs of the collision of the counter propagating streams of expanding plasmas upon explosion of a pair of silver wires (∅25 μm). The notation is the same as in Fig. 2.

3. Absorption of laser radiation and hydrothermal dissipation in the plasma of a metal droplet-vaporous medium

An analysis of the data presented in Section 2 points to the feasibility of model description of the medium which is formed upon the electric explosion of a thin wire in vacuum as an ensemble of droplets surrounded by vapour. The similarity of these media to the previously investigated volume-structured media can be considered as the starting point, taking into account, however, the presence of vapour.

Consider first the evolution of the low-density component of the medium upon laser irradiation. Because of the low initial density ($10^{18} - 10^{19}$ cm^{-3}), the vapour plays a minor part in the absorption of laser radiation. Indeed, the absorption coefficient (in cm^{-1}) due to inverse bremsstrahlung is (see, for instance, Ref. [5])

$$K_{ab} \approx 1.1 \times 10^7 \frac{\rho^2 \lambda^2}{T_e^{3/2}} \left(\frac{Z}{A}\right) Z, \tag{2}$$

where ρ is the plasma density (g cm^{-3}); λ is the wavelength (μm); T_e is the electron plasma temperature (keV); Z and A are the multiplicity and atomic weight of the plasma ions. Consider the heating of a metal vapour with an atomic weight $A = 100-200$ by the laser radiation with $\lambda = 1.06$ μm. For $\rho = 10^{-4}-10^{-3}$ g cm^{-3}, the electron plasma temperature may rise to $T_e \approx 1$ keV, which corresponds to ion charges $Z = 15 - 25$. It is easily seen from formula (2) that the absorption coefficient lies in the range $10^{-3}-10^{-2}$ cm^{-1}, and the vapour in such a medium measuring about 1 mm will therefore absorb only 0.1 %–1 % of the incident light energy. As a result, the absorption of laser radiation will take place primarily in the dense regions of the medium – first at the droplets due to the resonance absorption in the skin layer and then in the dense regions of the collisions of the plasma streams of expanding droplet. Nevertheless, although the vapour density is low, it is pertinent to note that its total mass is rather large and may be comparable with the mass of droplets under real experimental conditions. That is why the part played by the vapour in the transfer of absorbed laser energy may prove to be significant in the overall energy balance: the vapour-to-droplets mass ratio may be controlled over a rather wide range by varying the laser pulse delay relative to the wire explosion.

We now turn to the analysis of the features of plasma production upon laser irradiation of the dense components of the medium – metal droplets. From the previous Section it is known that the explosion products of a wire with a radius $r_w = 10$ μm occupy, in an expansion time $t_{ex} > 1$ μs, the cylindrical volume with a radius $a = 1 - 3$ mm. As a result, the average material density lowers by a factor $(a/r_w)^2$ from a value $\rho_s = 10$ g cm^{-3} typical for metals to $\rho_a = 10^{-3}$ g cm^{-3}. We estimate the droplet number density n_d and the average radius of medium cells r_c (half the interdroplet distance) from the expressions

$$n_d \approx \frac{3X}{4\pi r_d^3} \left(\frac{r_w}{a}\right)^2, \tag{3}$$

$$r_c \approx r_d \left(\frac{a}{r_w}\right)^{2/3} X^{-1/3}, \tag{4}$$

where X is the fraction of droplet material and r_d is the droplet radius. Putting $X = 0.8 - 0.9$, $r_d = 1 - 3$ μm, and $a/r_w = 100 - 300$, according to formulas (3) and (4) we find that $n_d = 5 \times 10^4 - 10^7$ cm^{-3} and $r_c = 30 - 100$ μm.

The absorption of laser radiation in the interaction with the droplets takes place over the geometric transparency depth of the medium. At the first stage of medium homogenisation, when the interdroplet space is initially filled with the plasma of vaporised droplets, it can be assumed that the geometric transparency depth is simply equal to the reciprocal of the product of the droplet cross section and the vapour number density [3]:

$$L_0 = \frac{4}{3X} r_d \left(\frac{a}{r_w}\right)^2 \equiv \frac{4}{3} r_d \frac{\rho_s}{X\rho_a}. \quad (5)$$

For the above medium parameters, the geometric transparency depth is 1–3 cm. It is comparable with the longitudinal target dimension and is 4–5 times larger than the transverse target size. In other words, during the first stage of homogenisation, an almost 100 % light absorption should be expected in the case of irradiation by a laser beam aligned with the discharge axis. Upon irradiation by a laser beam perpendicular to the target axis, the absorption amounts to 20 %–25 %.

The duration of the first (rapid) homogenisation stage is estimated from the ratio between the initial interdroplet distance and the front expansion velocity of exploded droplet material

$$t_1 = \frac{r_c}{v}. \quad (6)$$

The expansion velocity v is close to the sound velocity, which is easily estimated from the energy of laser radiation absorbed during the expansion

$$E = It_1 \pi r_{las}^2 \quad (7)$$

and the mass of substance in the geometric transparency region

$$M_s = \left(\frac{r_{las}}{r_d}\right)^2 \frac{4\pi}{3} r_d^3 \rho_s, \quad (8)$$

where r_{las} is the radius of the laser beam and I is the laser pulse intensity. According to these relations, the average energy per one particle (electron or ion) is

$$E_p = \frac{1}{C_V(\gamma - 1)} \left(\frac{3}{4} \frac{I}{\rho_s} \frac{r_c}{r_d}\right)^{2/3}, \quad (9)$$

where $C_V = (Z + 1)/(\gamma - 1)Am_p$ is the specific heat capacity (the temperature is expressed in energy units); γ is the adiabatic index; and m_p is the proton mass. Then,

$$t_1 = r_c \left(\frac{3}{4} \frac{I}{\rho_s}\right)^{-1/3} \left(\frac{r_d}{r_c}\right)^{1/3}. \quad (10)$$

For $I = 10^{14} - 10^{15}$ W cm^{-2} and the medium with the above parameters, $E_p = 1.5 - 6$ keV, and the first (rapid) homogenisation stage lasts for 300–600 ps.

The duration of the final second (slow) homogenisation stage, which eventually leads to the formation of a uniform plasma density distribution, is determined by the rate of viscous dissipation of the energy of colliding plasma streams and shock waves [6, 17]. The growth rate of the size of homogenised substance region is, by the order of magnitude, the ratio between the path for ion–ion collisions and the time the shock wave takes to travel the interdroplet distance. Hence the duration of the final homogenisation stage is [6, 17]

$$t_2 = \frac{r_c^2}{\lambda_{ii} V_s},$$

where λ_{ii} is the path for ion–ion collisions and V_s is the shock velocity. Exact calculations of the duration (in seconds) of the final homogenisation stage for a volume-structured material with solid spherical elements performed in Ref. [17] yielded the following result:

$$t_2 \approx 10^{-3} \frac{\rho_a r_c^2 Z^{5/2}}{T^{5/2}} \left(\frac{Z}{A}\right)^{1/2} \quad (11)$$

(here, ρ_a is measured in g cm^{-3}, r_c in cm, and T in keV).

The fast growth of the duration of the final homogenisation stage with increasing Z significantly lengthens the lifetime of the nonequilibrium plasma of metallic droplet-vaporous medium in comparison with the case of porous media of light elements. For the plasma with $r_c = 30$–100 μm and $\rho_a = 10^{-3} - 10^{-2}$ g cm^{-3} we are interested in, for a temperature of 1 keV (this corresponds to an ionisation multiplicity of 15–20) the duration of the final homogenisation stage is, according to formula (11), 10–50 ns, while for a porous polystyrene or agar–agar under the same parameters it is equal to 1–5 ns.

The collisions of plasma streams and shock waves generate during homogenisation time- and space-stochastic high-density plasma regions with an ion temperature significantly greater than the electron temperature. According to the calculations of Ref. [17], the average dimensions of such regions and their average plasma densities are

$$r_p = \frac{r_c}{(1 + \beta)^{3/2\beta}} \quad \text{and} \quad \rho_d = (1 + \beta)^{9/2\beta} \rho_a, \quad (12)$$

where $\beta = 3(\gamma - 1)(v + 1)/2$ is the kinetic-to-thermal energy ratio in the isothermal expansion of a given mass of material [18], and the values $v = 0, 1, 2$ correspond to plane, cylindrical, and spherical expansion.

For a spherical expansion, we assume that $\gamma = 5/3$ to obtain $r_p = r_c/2$ and $\rho_d = 8\rho_a$. The dimension of dense nonequilibrium plasma regions is equal to about half the interdroplet distance and the plasma density in these regions exceeds the average density by about an order of magnitude. As the plasma homogenises, the geometric transparency depth decreases owing to the increase of the dimensions of dense substance regions. The geometric transparency depth averaged over the homogenisation time can be calculated from the average dimension of the dense regions

$$L_g = \frac{4}{3} r_d \frac{r_d}{r_p} \frac{\rho_s}{X\rho_a}.$$

Hence, using formula (12) we obtain

$$L_g = \frac{8}{3} r_d \left(\frac{\rho_s}{X\rho_a}\right)^{1/3}. \quad (13)$$

A comparison of expressions (13) and (1) points to the significance of the geometrical structural factor: the geometric transparency depth in the partly homogenised plasma of the volume-structured substance with a droplet structure is less strongly dependent on the ρ_s/ρ_a density ratio than in a structurally fibrous substance. As a consequence, the geometric transparency depth during the long final homogenisation stage proves to be significantly [by a factor $(\rho_s/\rho_a)^{2/3}/2$] smaller than its initial value. For instance, for a ratio $\rho_s/\rho_a = 10^4$ and a droplet radius $r_d = 1 - 3$ μm it is equal to 100 – 300 μm.

Important conclusions on the nature and efficiency of laser radiation absorption in a porous medium produced in the electric explosion of thin wires can be drawn from the results of calculations of geometric transparency depth. Early in the homogenisation, the geometric transparency depth is large and comparable with the length of inverse bremsstrahlung of light in a plasma with a subcritical density of $10^{-4} - 10^{-3}$ g cm^{-3}. Any of these lengths exceeds the transverse target dimension by about an order of magnitude, and therefore the absorption of light takes place both in the subcritical plasma of the vapour and vaporised droplet material (the inverse bremsstrahlung mechanism) and in the non-vaporised parts of the droplets (the resonance mechanism), but the total absorption efficiency is not high.

Therefore, for laser pulses shorter than the 300 – 600 ps duration of initial homogenisation stage, the efficiency of radiation absorption does not exceed 10 % – 20 %. The geometric transparency depth of a partially homogenised plasma is 100 times smaller than the length of inverse bremsstrahlung of light in the subcritical-density plasma and is 10 times smaller than the transverse target dimension. For laser pulses longer than the initial homogenisation stage but shorter than the final homogenisation stage (10 – 50 ns), the absorption of laser radiation therefore takes place in volume over the geometric transparency depth of a partially homogenised plasma [see formula (13)] and the absorption efficiency is close to 100 %.

Because of density oscillations in the partially homogenised plasma, subcritical-density regions can occur even in the supercritical-density porous substance. As in the case with porous media of light elements, this is a prerequisite to the high efficiency of volume absorption of laser radiation in a metallic droplet-vaporous medium with a supercritical average density, which may exceed the critical density by an order of magnitude.

The collisions of plasma streams and shock waves, which are accompanied with hydrothermal dissipation, are the cause of the nonequilibrium state of the partially homogenised laser-produced plasma of porous media. In the expansion of dense particles of the porous substance, a large fraction of energy, which initially resides in the form of thermal electron energy, is converted to kinetic ion energy. As already noted, the kinetic-to-thermal energy ratio in the isothermal expansion of a spherical particle is $E_h/E_T = 3$. In the collision of hydrodynamic flows there occurs, on the contrary, the kinetic-to-thermal energy conversion. The electron – ion energy relaxation time far exceeds the ion relaxation time. In the course of hydrothermal dissipation in the collision of plasma streams, the energy of hydrodynamic motion therefore transforms to the thermal ion energy and only after that there occurs the ion-to-electron energy transfer in the plasma.

The calculation carried out in Ref. [3] for a porous material of light elements revealed a considerable difference between the relaxation times under discussion. For agar-agar with an average density of 10^{-3} g cm^{-3}, the ion – ion relaxation time was equal to 28 ps and the electron – ion relaxation time to 640 ps. In this case, the former time is significantly shorter than the period of collisions (100 – 200 ps) and the latter is significantly greater than that, which is the cause of nonequilibrium plasma formation with the predominant heating of the ion component. For the plasma of a metallic droplet-vaporous medium one would expect an even greater difference in the relaxation times due to the lengthening of the relaxation between electrons and heavier ions.

So, we assume that 3/4 of the energy is transferred to the energy of hydrodynamic ion motion and 1/4 to the electron and ion thermal energy as a result of expansion of the spherical droplets. Then, for the average kinetic energy of hydrodynamic ion motion E_h and the plasma particle temperature T_0 at the instant of collision of the plasma streams we have

$$E_h = \frac{3}{4}(Z+1)E_p, \tag{14}$$

and

$$T_0 = \frac{1}{4}(\gamma - 1)E_p. \tag{15}$$

Here, E_p is described by expression (9). The ion – ion and electron – ion relaxation times τ_{iiE} and τ_{eiE} are expressed in terms of the electron – ion collision time

$$\tau_{ei} = 3.4 \times 10^{-15}\frac{T_e^{3/2}A}{\rho Z^2}, \tag{16}$$

where the temperature T_e and the plasma density ρ are considered to mean, as applied to the problem involved, their values at the instant of collision, respectively T_0 and $8\rho_a$ [see formulas (12) and (15)].

Taking into account (14) and (15), we have

$$\tau_{eiE} = \left(\frac{m_i}{2m_e}\right)\tau_{ei} \approx 9 \times 10^2 A\tau_{ei}, \tag{17}$$

$$\tau_{iiE} = \frac{2^{1/2}}{Z^2}\left(\frac{m_i}{m_e}\right)^{1/2}\left(\frac{E_h}{T_e}\right)^{3/2}\tau_{ei} \approx 3 \times 10^2\left(\frac{A}{Z}\right)^{1/2}\tau_{ei}, \tag{18}$$

where $m_{e,i}$ are the electron and ion masses, respectively. Therefore,

$$\frac{\tau_{iiE}}{\tau_{eiE}} = \frac{1}{3}\frac{1}{A}\left(\frac{A}{Z}\right)^{1/2}.$$

This ratio clearly demonstrates that the excess of electron–ion time over the ion – ion time increases with the ionic atomic weight. A calculation of the relaxation times for $E_p = 1$ keV (which corresponds to $I = 10^{14}$ W cm^{-2}), $\rho_a = 10^{-3}$ g cm^{-3}, and $Z = 15 - 20$ yields the following results: $\tau_{eiE} = 4000$ ps and $\tau_{iiE} = 20$ ps. The ion – ion time is considerably shorter and the electron – ion time, on the contrary, is considerably longer than the period of plasma stream collisions (300 – 600 ps). That is why during both

homogenisation stages the plasma of a metallic droplet-vaporous medium will be in a nonequilibrium state with an ion temperature $T_i = (\gamma - 1)(1 + 3Z/4)E_p$ corresponding to the sum of the thermal and hydrodynamic ion energies at the instant of stream collision and an electron temperature $T_e = (\gamma - 1)E_p/4$. For $I = 10^{14}$ W cm^{-2}, the temperatures are $T_i = 8 - 12$ keV and $T_e = 0.2 - 0.3$ keV.

The effect of long lifetime of the nonequilibrium plasma of porous media with the predominant heating of the ion component underlies the proposal of developing a high-power neutron source with an intensity of 10^9 DT neutrons or 10^6 DD neutrons per Joule of laser energy deposition [2]. For a plasma produced in the electric explosion of a thin wire, the production of such a source may involve harnessing, as the exploding wire material, metals with the capacity to efficiently adsorb deuterium or tritium (such as palladium or platinum). The ion temperature of the laser-driven nonequilibrium plasma in relation to the mass content of deuterium or tritium ions in the conductor material will be

$$T_i = \frac{(\gamma - 1)\bar{E}_p}{4}\left[1 + 3(Z_m + 1)\left(\frac{A_f}{A_m}\frac{\mu_m}{\mu_f} + \frac{Z_f + 1}{Z_m + 1}\right)\right.$$
$$\left.\times\left(\frac{A_f}{A_m}\frac{\mu_m}{\mu_f} + 1\right)^{-1}\right], \qquad (19)$$

where $A_{m,f}$, $Z_{m,f}$, and $\mu_{m,f}$ are the atomic weight, the ionisation multiplicity, and the mass content of the metal ions or the ions of light elements, respectively; $\bar{E}_p$ is the average energy per particle,

$$\bar{E}_p = \frac{1}{(\gamma - 1)\tilde{C}_V}\left[\frac{3}{4}\frac{I}{\rho_m(1 + \mu_f/\mu_m)}\frac{r_c}{r_d}\right]^{2/3}; \qquad (20)$$

ρ_m is the metal density; and $\tilde{C}_V$ is the specific heat capacity of the composition medium,

$$\tilde{C}_V = \left[(Z_m + 1) + (Z_f + 1)\frac{A_m}{A_f}\frac{\mu_f}{\mu_m}\right][(\gamma - 1)A_m m_p]^{-1}.$$

Note that expression (19) is transformed into $T_i = (\gamma - 1)(1 + 3Z/4)E_p$ in the limit $\mu_f \to 0$.

As the relative content of light nuclei increases, the ion temperature decreases. However, under laser pulse irradiation at $I = 10^{15}$ W cm^{-2} it is possible to attain fusion ion temperatures for metals with a rather high content of light nuclei. For instance, for deuterium-bearing palladium ($A = 106$, $Z_a = 46$) and an equal mass content of the nuclei of both elements $\mu_D = \mu_{Pd}$, the temperature of deuterium nuclei, according to formula (14), for $Z = 15$ amounts to only 2 keV at an intensity $T = 10^{14}$ W cm^{-2} but amounts to 8–10 keV at 10^{15} W cm^{-2}.

4. Energy transfer in the laser plasma of a metallic droplet-vaporous medium

Unlike the plasma of the porous media of light elements with empty cellular space, in the plasma of metallic droplet-vaporous medium, where the interdroplet space is filled with vapour, there exist prerequisites for the efficient action of all kinds of energy transfer, including the radiative mechanism and the electron thermal conduction. To estimate the role of electron thermal conduction in the plasma of a porous medium, the characteristic temperature gradient is determined from the temperature variation across the interdroplet distance r_c. In this case, for the velocity of electron thermal conduction wave we obtain

$$V_\kappa = \frac{\kappa_0 T^{7/2}}{C_V \rho r_c},$$

where $\kappa_0 \approx 10^{19}/Z$ is the coefficient characterising the electron heat conductivity (see, for instance, Ref. [1]). For the interdroplet vapour plasma with the parameters $T = 0.5 - 1$ keV, $\rho = 10^{-3} - 10^{-2}$ g cm^{-3}, and $Z = 10$–15, the values of V_κ prove to lie in the $10^7 - 10^8$ cm s^{-1} range, which exceeds the sound velocity. This has the following implication: while the electron thermal conduction wave in the plasma of porous media with empty cellular space can emerge only after the hydrodynamic perturbation front (which provides the production of free electrons in the cellular volume), in the above-considered medium with vapour in the space between the droplets there occurs an independent mechanism of electron thermal conduction. This mechanism proves to be even more significant than the hydrodynamic energy transfer.

We perform a qualitative analysis of radiative energy transfer employing approximate analytic relations for the Rosseland radiation lengths. For the plasmas of several metals they can be found, for instance, in Refs [19, 20]. In particular, the Rosseland length (in cm) in the gold plasma is [19]

$$\lambda_R = 10^{-2}\frac{T^{2.5}}{\rho^{1.5}}$$

(T is measured in keV and ρ in g cm^{-3}). By comparing the Rosseland length with the smallest of medium dimensions – the transverse dimension equal to $a = (1 - 3) \times 10^{-1}$ cm – it is easy to understand that the radiative thermal conduction wave is formed provided that the radiation is equilibrium ($\lambda_R \ll a$), which is fulfilled for the gold plasma when

$$\rho > (0.1 - 0.2)T^{5/3}. \qquad (21)$$

Furthermore, it is clear that one would expect a high degree of conversion of absorbed laser radiation energy to soft X-ray energy precisely when the condition of equilibrium radiation state is fulfilled. For a pulsed plasma, one more condition for the high degree of conversion of the energy inputted into the plasma to the intrinsic radiation energy is that the energy losses for hydrodynamic substance motion are small in comparison with the intensity of radiative processes. The longer is the plasma, the more safely is this condition fulfilled [19]. As shown in Ref. [4], the condition that the energy expenses for hydrodynamic motion are low is fulfilled on precisely the scales that correspond to the typical transverse dimension of the plasma resulting from the electric explosion of a thin wire $a = 0.1 - 0.3$ cm. By way of example we give the parameters of a low-density gold plasma for $a \geqslant 0.1$–0.3 cm, which correspond to efficient radiative energy transfer and a high (close to 100 %) laser-to-soft X-ray conversion efficiency: for a temperature $T = 0.5$ keV, the plasma density should exceed 0.03–0.06 g cm^{-3}, and A similar analysis for a copper plasma [20], where

$$\lambda_R = 3.2 \times 10^{-2} \frac{T^{2.77}}{\rho^{1.72}},$$

yields the following results: $T = 0.5$ keV, $\rho > 0.05-0.1$ g cm^{-3}, and $T = 0.2$ keV requires $\rho > 0.01 - 0.02$ g cm^{-3}.

The above estimates show that the metallic droplet-vaporous medium arising from the electric explosion of a thin wire is a target which by its parameters satisfies the requirements for the development of a high-power pulsed soft X-ray source.

5. Conclusions

The metallic droplet-vaporous medium emerging in the electric explosion of a thin wire is an interesting object of research from the viewpoint of production of nonequilibrium metallic plasma upon irradiation of this medium by a high-power laser pulse with an intensity of $10^{14} - 10^{15}$ W cm^{-2}. Due to the high ion charge, the departure from the state of plasma equilibrium in such media proves to be much stronger compared to the laser plasma of the porous media of light elements. In particular, the complete homogenisation time for the plasma of metallic droplet-vaporous medium ranges into the tens of nanoseconds. The stochastically produced dense plasma regions, which exist for several hundred picoseconds with predominant ion heating, are characterised by a significant difference between the ion and electron temperatures: $T_i = 10 - 30$ keV for $T_e = 0.3 - 0.6$ keV.

When a laser pulse with $I = 10^{14} - 10^{15}$ W cm^{-2} irradiates a porous metallic medium produced in the electric explosion of a thin wire, the attainable laser-to-soft X-ray energy conversion efficiency may be close to unity. By employing a metal with internally adsorbed deuterium and tritium nuclei as the exploded conductor material, it is possible to produce a high-power source of fusion neutrons driven by a laser pulse with an intensity of the order of 10^{15} W cm^{-2}.

It is significant that the average density of the droplet-vaporous medium produced in the explosion of wires may vary over a very wide range. It is easily lowered by the proper choice of the expansion time after the cessation of the current pulse. In particular, it is possible to overcome the limitation on the medium density (0.1 g cm^{-3}) caused by the necessity of providing the rigidity of the porous metallic media with open pores, which is encountered in their fabrication by the foaming technique. Also absent in this case are the technological difficulties associated with the fabrication of artificial fibrous media of thin metallic filaments (the restrictions on exploding-wire thickness are less stringent). When the droplet-vaporous medium is used, the presence of metal vapour in the interdroplet space will not impede attaining high ion temperatures, either: as shown in our paper, the laser beam will interact primarily with the substance of the droplets. All this gives promise that the proposed method will be expedient to harness.

Acknowledgements. This work was supported by the ISTC under Grant No. 2151.

References

1. Gus'kov S.Yu., Zmitrenko N.V., Rozanov V.B. *Zh. Eksp. Teor. Fiz.*, **106**, 548 (1995).
2. Gus'kov S.Yu., Zmitrenko N.V., Rozanov V.B. *Pis'ma Zh. Eksp. Teor. Fiz.*, **66** (8), 521 (1997).
3. Gus'kov S.Yu., Rozanov V.B. *Kvantovaya Elektron.*, **24** (8), 715 (1997) [*Quantum Electron.*, **27** (8), 696 (1997)].
4. Gus'kov S.Yu., Merkul'ev Yu.A. *Kvantovaya Elektron.*, **31** (4), 311 (2001) [*Quantum Electron.*, **31** (4), 311 (2001)].
5. Bugrov A.E., Burdonskii I.N., Gavrilov V.V., et al. *Zh. Eksp. Teor. Fiz.*, **111**, 903 (1997).
6. Bugrov A.E., Burdonskii I.N., Gavrilov V.V., et al. *Zh. Eksp. Teor. Fiz.*, **115**, 805 (1999).
7. Caruso A., Gus'kov S.Yu., Demchenko N.N., et al. *J. Rus. Las. Res.*, **18**, 464 (1997).
8. Gus'kov S.Yu., Caruso A., Rozanov V.B., Strangio C. *Kvantovaya Elektron.*, **30** (3), 191 (2000) [*Quantum Electron.*, **30** (3), 191 (2000)].
9. Ditmire T., Donnelly T., Rubenchik A.M., et al. *Phys. Rev. A*, **53**, 3379 (1996).
10. Sinars D.B., Min Hu, Chandler K.M., et al. *Phys. Plasmas*, **8**, 216 (2001).
11. Sinars D.B., Shelkovenko T.A., Pikuz S.A., et al. *Phys. Plasmas*, **7**, 429 (2000).
12. Pikuz S.A., Ivanenkov G.V., Shelkovenko T.A., Hammer D.A. *Pis'ma Zh. Eksp. Teor. Fiz.*, **69**, 349 (1999).
13. Pikuz S.A., Shelkovenko T.A., Greenly J.B., Dimant Y.S., Hammer D.A. *Phys. Rev. Lett.*, **83**, 4313 (1999).
14. Shelkovenko T.A., Pikuz S.A., Mingaleev A.R., Hammer D.A. *Rev. Sci. Instr.*, **70**, 667 (1999); Shelkovenko T.A., Sinars D.B., Pikuz S.A., et al. *Rev. Sci. Instr.*, **72**, 667 (2001).
15. Pikuz S.A., Romanova V.M., Baryshnikov N.V., et al. *Rev. Sci. Instr.*, **72**, 1098 (2001).
16. Pikuz S.A., Shelkovenko T.A., Mingaleev A.R., Hammer D.A., Neves H.P. *Phys. Plasmas*, **6**, 4272 (1999).
17. Gus'kov S.Yu. Preprint FIAN (49), 1999.
18. Imshennik V.S. *Dokl. Akad. Nauk SSSR*, **131**, 1287 (1960).
19. Vergunova G.A., Rozanov V.B. *Kvantovaya Elektron.*, **19** (3), 263 (1992) [*Sov. J. Quantum Electron.*, **22** (3), 239 (1992)].
20. Minguez E., Munoz R., Ruiz R., et al. *Laser and Particle Beams*, **17** (4), 799 (1999).